BNL-209040-2018-TECH

CBETA/020

Status of the CBETA splitter common magnet design

J. Crittenden, S. Peggs

September 2017

Collider Accelerator Department

Brookhaven National Laboratory

U.S. Department of Energy

USDOE Office of Science (SC), Nuclear Physics (NP) (SC-26)

Notice: This technical note has been authored by employees of Brookhaven Science Associates, LLC under Contract No.DE-SC0012704 with the U.S. Department of Energy. The publisher by accepting the technical note for publication acknowledges that the United States Government retains a non-exclusive, paid-up, irrevocable, world-wide license to publish or reproduce the published form of this technical note, or allow others to do so, for United States Government purposes.

DISCLAIMER

This report was prepared as an account of work sponsored by an agency of the United States Government. Neither the United States Government nor any agency thereof, nor any of their employees, nor any of their contractors, subcontractors, or their employees, makes any warranty, express or implied, or assumes any legal liability or responsibility for the accuracy, completeness, or any third party's use or the results of such use of any information, apparatus, product, or process disclosed, or represents that its use would not infringe privately owned rights. Reference herein to any specific commercial product, process, or service by trade name, trademark, manufacturer, or otherwise, does not necessarily constitute or imply its endorsement, recommendation, or favoring by the United States Government or any agency thereof or its contractors or subcontractors. The views and opinions of authors expressed herein do not necessarily state or reflect those of the United States Government or any agency thereof.

Status of the CBETA Splitter Common Magnet Design

J.A. Crittenden,* R.M. Bass, D.A. Burke, and K.W. Smolenski
CLASSE, Cornell University, Ithaca, NY 14853, USA
(Dated: September 8, 2017)

The two common dipole magnets in each of the two CBETA splitter sections serve to direct the beams of 42, 78, 114 and 150 MeV from the linac or FFAG return loop exit into the separate splitter lines for path length adjustment and to direct the beams from the splitter into the linac or FFAG return loop entrance. Here we report the results of design and tracking studies based on the Opera V18R2 software. The choice of the H-magnet design included consideration of using the coil design developed for the internal splitter H-dipoles by Elytt Energy. Considerations of transverse space constraints and the bend angle of about 30 degrees for the 42-MeV beam led to the adoption of a T-shape for the pole. The XYZ magnet dimensions are $34 \times 42 \times 16$ cm. The central field value is 3.6-3.9 kG, but the magnet can operate as high as 4.9 kG, allowing for tests of a beam energy as high as 54 MeV in the S1 splitter line. We include results of tracking studies showing optimal placement of the magnets based on bend angle uniformity for the four beam energies. The project now proceeds to the full engineering design and fabrication to be performed by Elytt Energy.

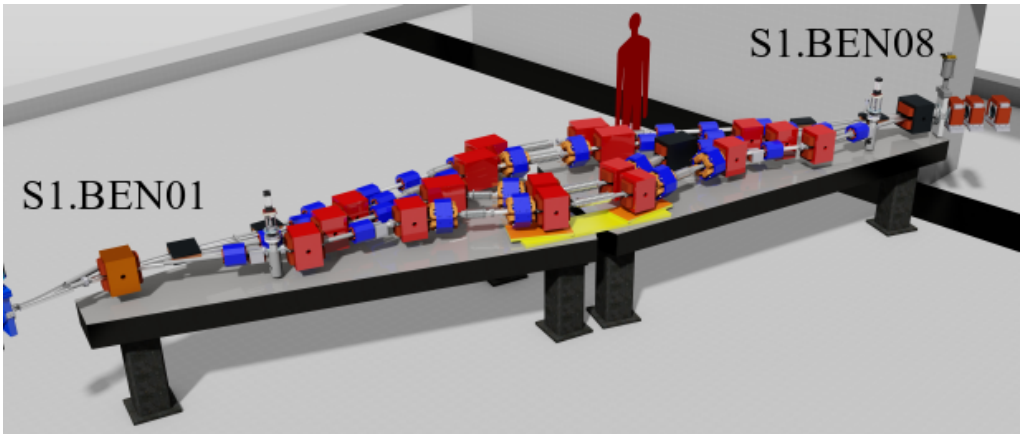

* E-mail: crittenden@cornell.edu

I. INTRODUCTION

The Cornell-Brookhaven Energy-recovery-linac Test Accelerator (CBETA) [1] project is in the design phase of a four-pass 150-MeV electron accelerator based on energy recovery in a superconducting linear accelerator and a fixed-field alternating-gradient (FFAG) return loop. Optics matching and path length adjustment between the linear accelerator and the FFAG return loop sections is accomplished using four beamlines in each of two splitter sections, as shown in Fig. 1.

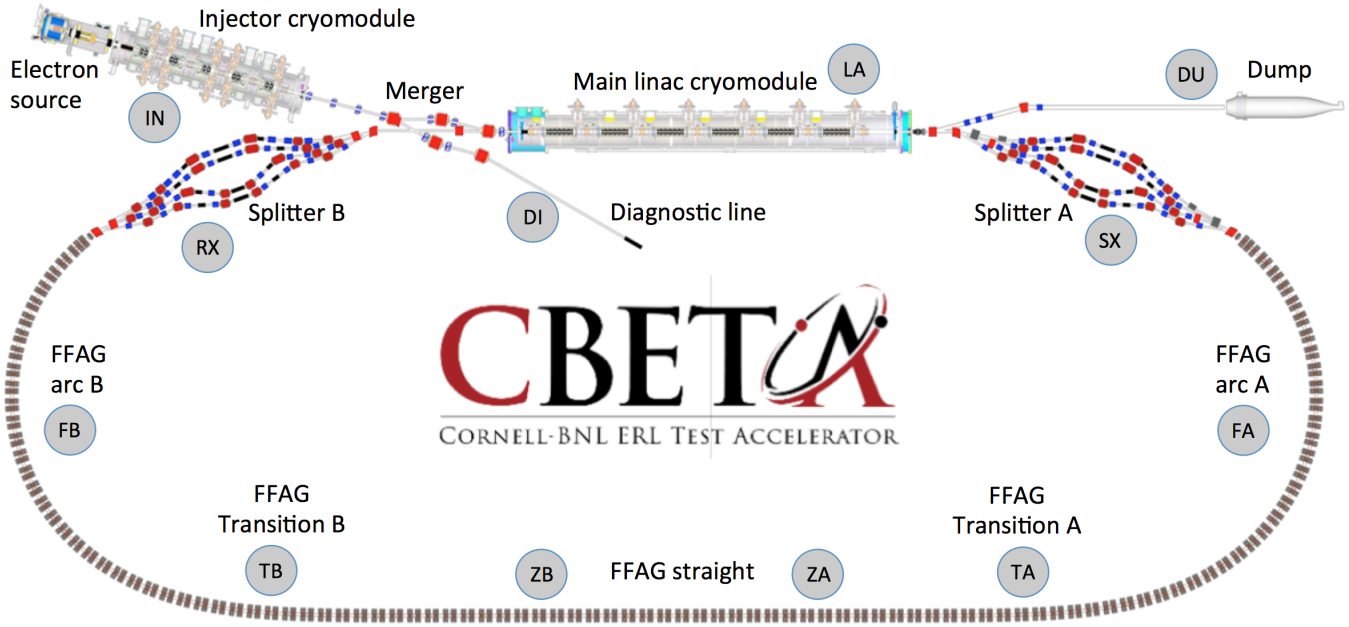

FIG. 1. Complete CBETA layout. The RX and SX splitter sections are upstream and downstream of the linear accelerator cryomodule, respectively.

The range of operating parameters for the common, septum and H-dipole magnets in the splitters are shown in Table I. The lattice design values for the common magnets are shown in Table II.

A comprehensive tracking study [2] based on OPERA [3] modeling results was performed for the H-dipoles during the summer of 2017, providing information on optimal placement of the magnets relative to the four beam trajectories. This project included a preliminary assessment of the bend angle uniformity and optimal placement of the S1.BEN01 common magnet. The present report complements that study with results for all four of the common magnets, and includes an assessment of the operating limit of the magnet for purposes of using the S1 line as a measurement for acceptance of energies higher than 42 MeV. The common magnets serve to guide the four beams from/to the linac into the splitter beamlines and to/from the FFAG return loop. The trajectories of each beam in each of the four common magnets are shown in Fig. 2. The difference in transverse position between the 42- and 150-MeV beams indicates the challenge in field quality that these magnets must satisfy [4]. While cost and simplicity considerations motivate a single design for the four common dipoles, it is to be noted that the transverse range of good field quality is much wider in the R/S1.BEN08 magnets, since the trajectory separations are much larger (approximately 40 mm rather than 10 mm.) An additional consideration is the space constraint imposed by the 6-MeV beam dump line following the final pass through the linear accelerator. The proximity of the dump line requires cutting off a corner of the S1.BEN01 common magnet steel by an amount determined by the present tracking study.

II. OPERA 3D DESIGN

The magnet design and tracking studies were performed with version 18R2 of the Opera 3D finite-element, solver and post-processing software [3]. The finite-element mesh cell sizes were 4 mm in the region of the beam, 16-mm in the yoke and 1-mm in the pole face steel. Figure 4 shows the results of tracking 42-MeV electrons through the magnet field of a model with the design excitation of the S1.BEN01 magnet, 5826 amp-turns. For clarity, the coils are not shown. The color contours show the ratio of the magnetic flux B to the magnetic field H on the steel surface,

TABLE I. September 6, 2017 - Range of operational parameters for the CBETA splitter dipole and common Magnets. These values are defined by the lattice design of 10 April 2017. They include the required adjustment margins on the maximum field values of 10%.

Parameter	**H-Dipole 21x31x16**	**H-Dipole 21x31x24**	**H-Dipole 21x31x31**	**Common 34x42x16**	**H-Dipole 15x28x10**
JAC OPERA model version number	33	33	33	39	4
Number of magnets	24	4	8	4	8
Gap or Bore (cm)	3.6	3.6	3.6	3.6	3.6
Steel height (cm)	30.5	30.5	30.5	42.0	28.0
Steel width (cm)	21.0	21.0	21.0	34.0	15.0
Steel length (cm)	16.0	24.0	31.0	16.0	10.0
Width including coil (cm)	21.0	21.0	21.0	34.0	15.0
Length including coil (cm)	24.1	37.4	37.4	24.1	20.0
Pole width (cm)	7.66	7.66	7.66	19.66	4.50
Field (T)/Gradient (T/m)	0.230-0.602	0.623-0.655	0.424-0.670	0.399-0.432	0.070-0.479
Field Integral (T-m) at X = 0 cm	0.046-0.120	0.177-0.185	0.146-0.231	0.081-0.087	0.007-0.048
Good Field Region (mm)	± 15	± 15	± 15	± 50	± 7
Central Field Uniformity* (%)	± 0.1	± 0.1	± 0.1	± 0.1	± 0.1
Field Integral Uniformity* (%)	± 0.1	± 0.1	± 0.1	± 0.5	± 0.1
Bend Angle Uniformity* (%)	± 0.1	± 0.1	± 0.1	± 0.5	± 0.1
NI per coil (Amp-turns)	3422-8972	9282-9667	6281-9918	6001-6505	1033-7079
Turns per coil	4 x 13				4 x 15
Coil cross section (cm x cm)	2.85 x 10.55				2.20 x 8.30
Conductor cross section (cm x cm)	(0.56x0.61)/0.36-cm diam hole				
Conductor straight length (cm)	16.4	29.8	29.8	16.4	9.0
Coil inner corner radius (cm)	1.40	0.84	0.84	14.	0.5
Conductor length per turn, avg (cm)	59.78	86.4	86.4	69.8	44.1
R_{coil} (Ω)	0.0229	0.0330	0.0330	0.0267	0.0317
L (mH)	2 x 10.0 = 20.0	2 x 13.8 = 27.6	2 x 17.0 = 34.0	2 x 23.5 = 47.1	41 x 3.2 = 6.4
Power supply current (A)	65.8-172.5	178.5-185.9	120.8-190.7	115.4-125.1	17.2-118.0
Current density (A/mm^2)	2.85-7.46	7.72-8.04	5.22-8.25	4.99-5.41	0.69-4.7
Voltage drop/magnet (V)	3.0-7.9	11.8-12.3	8.0-12.6	6.2-6.7	1.1-7.5
Power/magnet (W)	198-1364	2103-2281	963-2401	711-836	19-883

* Defined as horizontal deviation from the ideal field $(B_Y - B_Y^{\text{ideal}})/B_Y^{\text{ideal}}$.

TABLE II. Design values for the splitter common magnets. The values are defined by the lattice design of 10 April 2017. The field integral values are used to calculate the required excitation current.

splitter_common_magnets_4pass_20170410.table.txt Wed Sep 06 14:28:51 2017 1

	Type	S Position (m)	Length (m)	Momentum (MeV)	B field (T)	B integral (T-m)	Bd angle (degrees)	Bd Radius (m)	Sagitta (cm)	Gradient (T/m)	L (mH)	NI kA-turns	Power Supply (V)	(A)	Curr Density A/mm^2
1	S1.BEN01 H-common	23.150	0.160	41.997	-0.393	-0.079	32.487	0.283	1.127	0.000	47.10	-5.91	-6.1	-113.7	-4.92
8	S1.BEN08 H-common	30.733	0.160	41.997	-0.363	-0.073	30.023	0.306	1.043	0.000	47.10	-5.46	-5.6	-104.9	-4.54
17	R1.BEN08 H-common	79.701	0.160	41.997	-0.363	-0.073	30.023	0.306	1.043	0.000	47.10	-5.46	-5.6	-104.9	-4.54
24	R1.BEN01 H-common	87.334	0.160	41.997	-0.363	-0.073	30.023	0.306	1.043	0.000	47.10	-5.46	-5.6	-104.9	-4.54

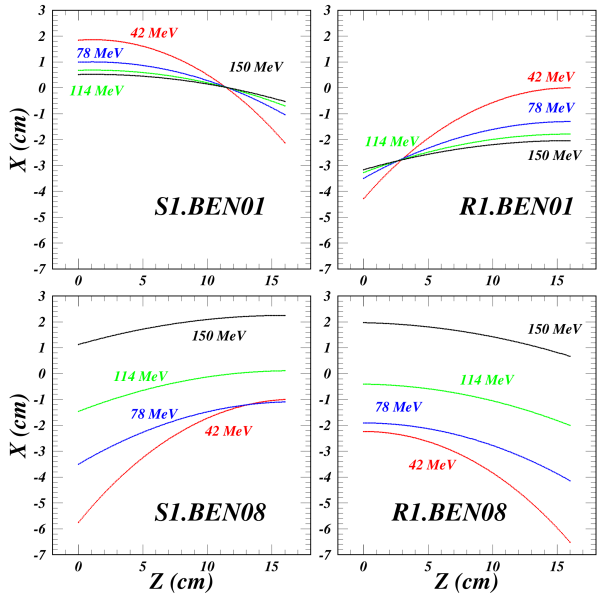

FIG. 2. Beam trajectories through common magnets in each location. The center of the magnet is at $X = 0, Z = 8$ cm.

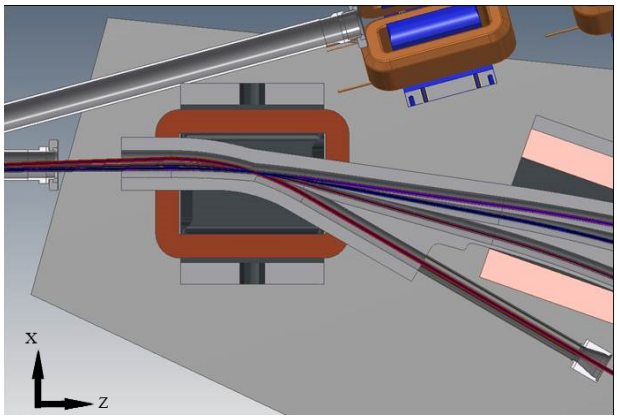

FIG. 3. The S1.BEN01 magnet and nearby dump line vacuum chamber for the 6 MeV beam. This pipe constrains the size and position of the S1.BEN01 magnet. The common magnets are oriented such that the magnet axis is parallel to the incoming beams, in the case of S1.BEN01 and R1.BEN08, or to the outgoing beams, as with S1.BEN08 and R1.BEN01.

indicating regions where saturation occurs. The design is similar to that of the internal splitter dipoles, but since the required range of fields is much smaller and the field uniformity specifications more stringent, the pole face is wider (19.7 cm instead of 7.7 cm) and, unlike the internal H-dipoles, larger than that of the pole stem (12.7 cm).

III. EXCITATION LIMIT

Figures 5 show the central field value and the central field integral values as a function of the excitation current. The design excitation value for the S1.BEN01 magnet is shown in red and that for the other three common magnets in magenta. The upper plots show the central value of the magnetic flux density B(X=Y=0,Z=8 cm) (left) and the longitudinal field integral (right). The lower plots show the relative deviation in those values from the low-excitation linear extrapolation. At an excitation 50% higher than the design value for S1.BEN01, the central field is only 18% higher, indicating that the operational limit of the magnet is reached. The tracking study shown in Sect. IV shows that a beam energy as high as 54 MeV can be accommodated in the S1 line.

IV. TRACKING STUDY AND OPTIMAL PLACEMENT

Electron tracking studies were undertaken for each of the four beam energies in each of the four common magnets. Figure 6 shows the results for the 42- and 150-MeV bend angle uniformity for the common magnet at the exit of the linac, S1.BEN01, and the exit from the FFAG loop, R1.BEN08, where the beam trajectories enter the magnet parallel to the magnet axis. Figure 7 show the results for the bend angle uniformity for the common magnet at the entrance to the FFAG loop, S1.BEN08, and the entrance to the linac, R1.BEN01, where the beam trajectories exit

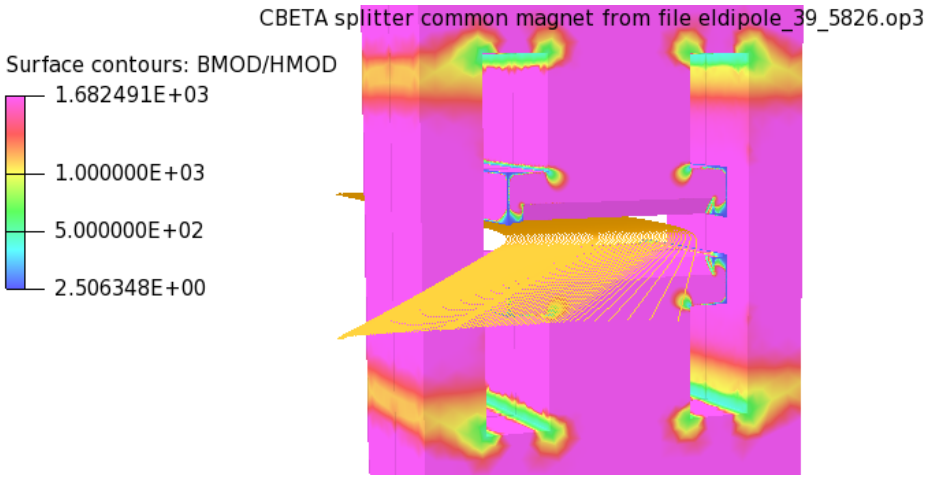

FIG. 4. Opera graphic showing tracking of 42-MeV electrons through the model for the S1.BEN01 common magnet excited to 5826 amp-turns. The two coils are not shown. The trajectories are parallel to the magnet axis upon entry, and the horizontal entry position varies from -80 to +80 mm.

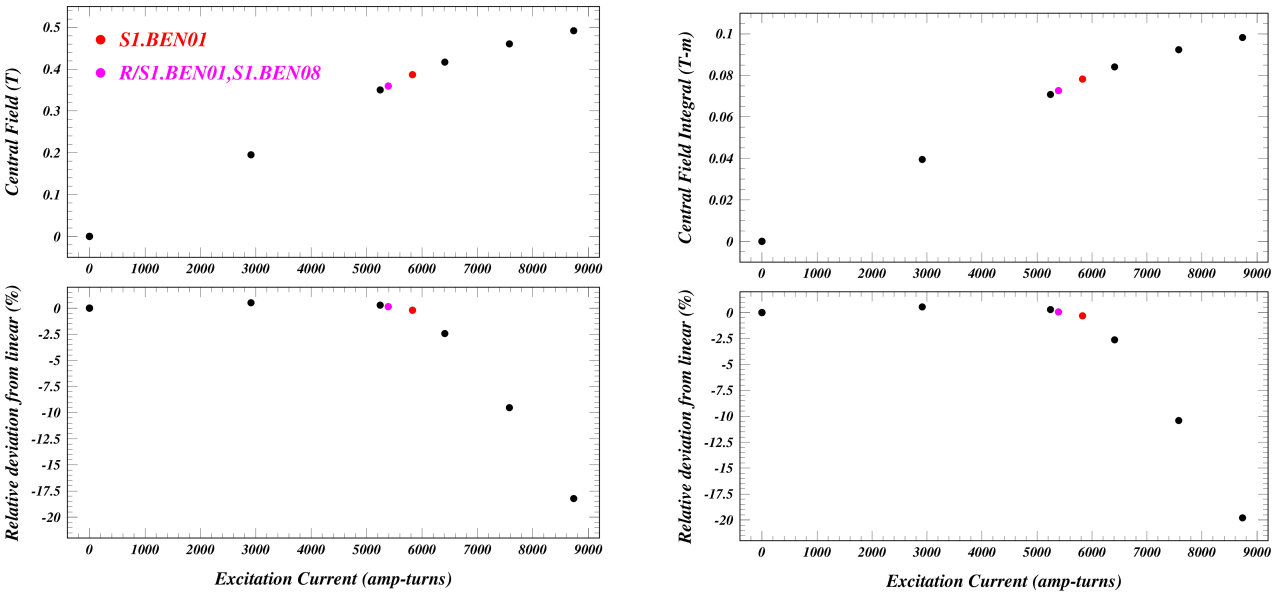

FIG. 5. Saturation limits for the splitter common magnet design. The top plots show the central value of the magnetic flux density B(X=Y=0,Z=8 cm) (left) and the longitudinal field integral (right). The lower plots show the relative deviation in those values from the low-excitation linearity.

the magnet parallel to the magnet axis. The relative bend angle deviation is shown as a function of the trajectory horizontal position at the longitudinal center of the magnet, with X=0 on the magnet axis. The relative positions of the 42- and 150-MeV beams at the magnet center are derived from the trajectories shown in Fig. 2. The vertical green lines show the optimized placement of the beams relative to the magnet axis.

The excitation currents of the magnets (5826 amp-turns for S1.BEN01 and 5393 amp-turns for the others) were chosen to optimize the region of good uniformity for the 42 MeV beams. As a consequence, the bend angles for the 150-MeV beams are 3-4% lower than in the lattice design, since the straighter trajectories sample less field. This orbit error must be compensated using the other magnets in the splitter lines.

The vertical blue lines in these figures show the positions of the interior vacuum chamber walls when the magnet is centered on the beampipe, i.e. prior to optimized placement. At the ends of the linac, the vacuum chamber width is chosen by the separation of the beams and the requirement of 12-mm beam clearance to the walls. Since the beam separation is 13 mm in S1.BEN01 and 20 mm in R1.BEN01, we have chosen a 44-mm width for both cases. At the return-loop ends, the width is chosen according to the nearby gate valve, which is 63 mm wide.

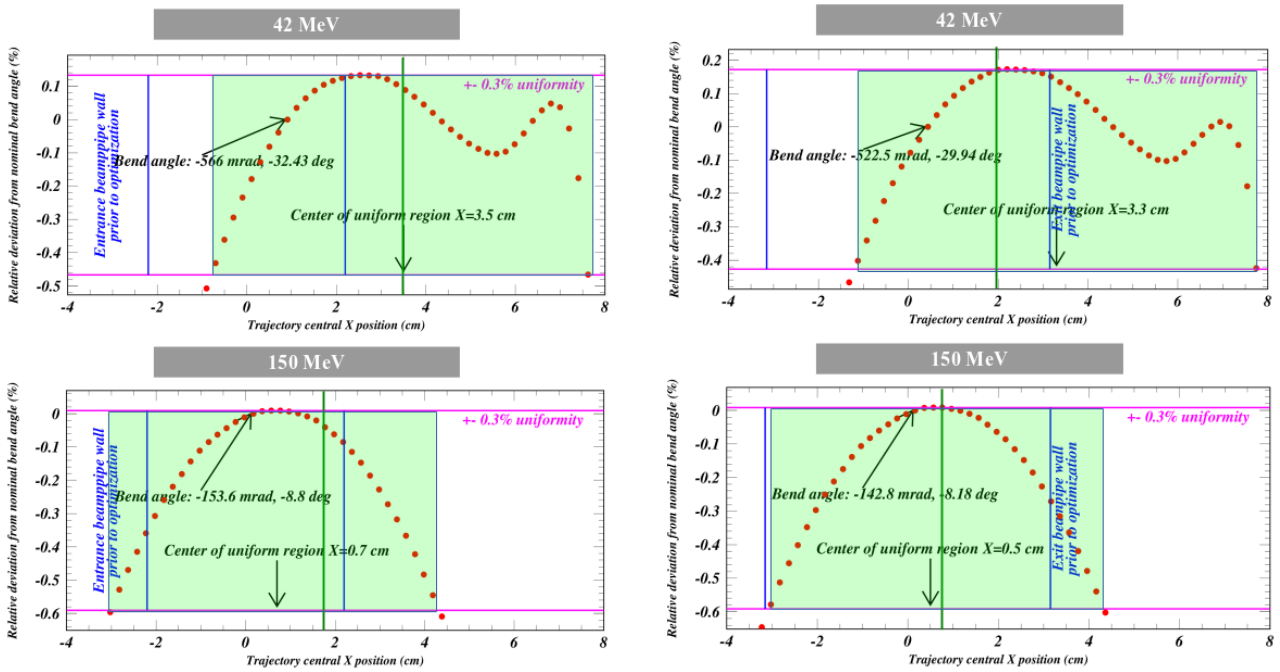

FIG. 6. Bend angle uniformity for S1.BEN01 (left) and R1.BEN08 (right) common magnets as functions of the horizontal trajectory position at the longitudinal center of the magnet for the 42- (top) and 150-MeV (bottom) beams. The beams enter these magnets parallel to the magnet axis. The vertical blue lines indicate the locations of the vacuum chamber wall at the entrance prior to optimal placement of the magnet. The green shaded areas indicate the region over which the bend angle varies by less than 0.5%.

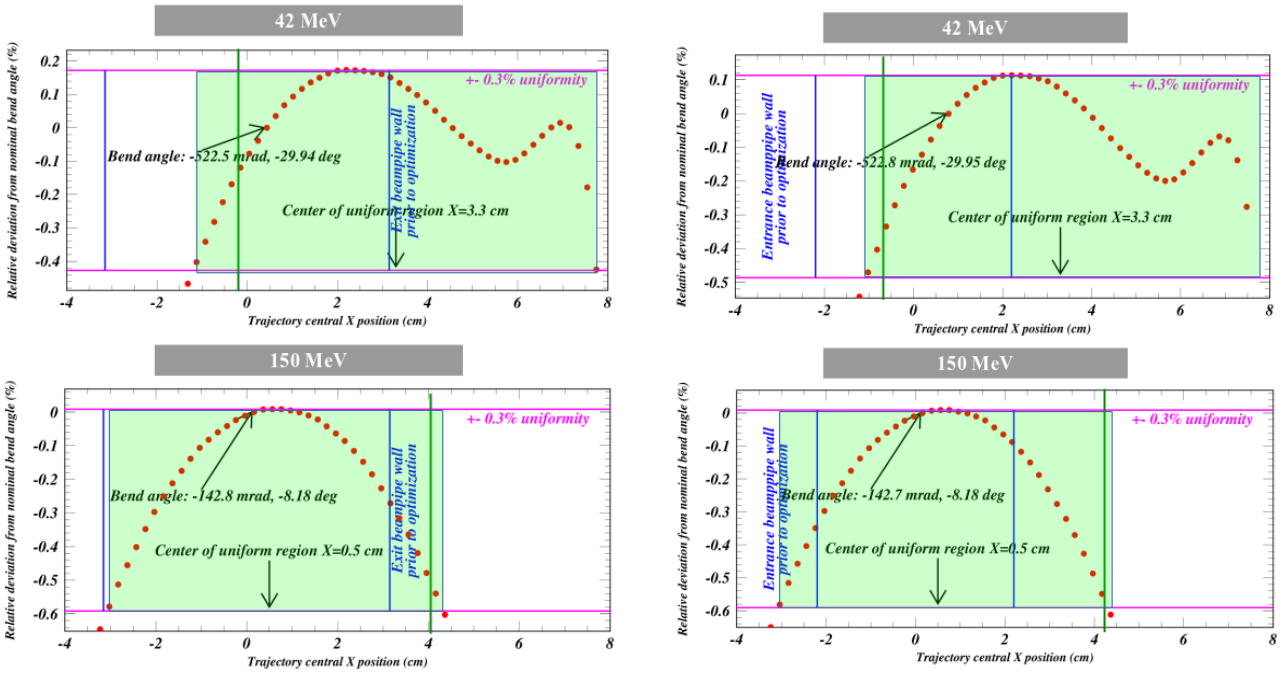

FIG. 7. Bend angle uniformity for S1.BEN08 (left) and R1.BEN01 (right) common magnets as functions of the horizontal trajectory position at the longitudinal center of the magnet for the 42- (top) and 150-MeV (bottom) beams. The beams exit these magnets parallel to the magnet axis. The vertical blue lines indicate the locations of the vacuum chamber wall at the exit prior to optimal placement of the magnet. The green shaded areas indicate the region over which the bend angle varies by less than 0.5%.

Table III summarizes the results of the tracking study determining the optimal transverse placement of the common magnets based on bend angle uniformity. The displacements range from 10 to 33 mm toward the inside of the CBETA ring.

TABLE III. Summary table of magnet placement optimization derived from the tracking studies

	S1.BEN01	S1.BEN08	R1.BEN08	R1.BEN01
Central X positions of the 42- and 150-MeV beams relative to the magnet axis (cm)	42 MeV: 3.5 150 MeV: 2.8	42 MeV: -0.2 150 MeV: 4.0	42 MeV: -0.7 150 MeV: 4.2	42 MeV: 2.0 150 MeV: 0.7
Transverse displacement to place beams (cm)	-2.45	-2.02	-3.25	-0.98
Bend angle (degrees)	42 MeV: 32.46 150 MeV: 8.79	42 MeV: 29.91 150 MeV: 8.14	42 MeV: 29.86 150 MeV: 8.13	42 MeV: 30.0 150 MeV: 8.18
Bend angle deviation (%)	42 MeV: +0,3, -0.3 150 MeV: +0.0, -0.6	42 MeV: +0,3,-0.3 150 MeV: +0.5, -0.1	42 MeV: +0,5, -0.1 150 MeV: +0.6, -0.0	42 MeV: +0,3, -0.3 150 MeV: +0.0, -0.6
Region of bend angle deviation (cm)	42 MeV: -4.2, 4.2 150 MeV: -7.0, +0.3	42 MeV: -1.0, +7.9 150 MeV: -7.0, +0.3	42 MeV: -0.3, +8.4 150 MeV: -7.2, +0.2	42 MeV: -3.2, +5.7 150 MeV: -3.7, +3.5

The tracking study for S1.BEN01 was extended to an excitation 50% higher than nominal, as described in Sect. III, 8739 amp-turns. Figure 8 shows the resulting bend angle uniformity as a function of entrance position for a 54 MeV beam. Comparison to the result in Fig. 6 shows that the region of ±0.3% relative deviation from the nominal bend angle is reduced only slightly, from a width of 76 mm to 71 mm.

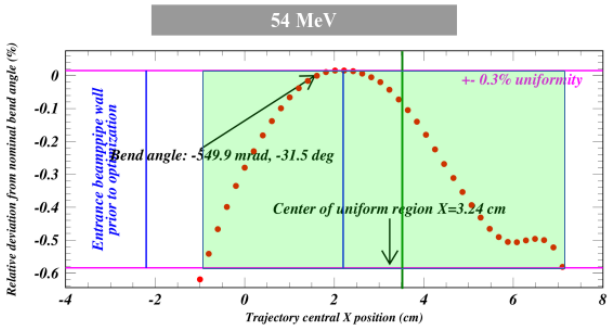

FIG. 8. Bend angle uniformity for S1.BEN01 at an excitation of 8739 amp-turns to direct a 54-MeV beam into the S1 line from the linac.

The primary conclusion of the tracking study is that the field quality of this design for the common magnet suffices to provide the nominal bend angles accurate to +-0.3% for all beams over a region approximately 70-mm wide in horizontal entrance position. When the excitations are chosen to give the nominal design bend angle for the 42-MeV beam, the bend angles for the higher energy beams can deviate from the nominal values by as much as 4%.

V. CONCLUSION

We have concluded a preliminary design study including trajectory calculations for the four common magnets in the splitter regions of the CBETA test accelerator. The design pole face width of 19.7 cm suffices to provide deflection angles varying by less than ±0.3% over a 70-mm-wide region of entrance position for all beams in all magnets. When the magnet strengths are chosen to give the design deflection for the 42-MeV beam, the bend angles for the other beams can be as much as 4% lower than nominal. Saturation effects related to flux leakage from the central pole and saturation in the return yoke limit the maximum central field value to about 4.9 kG. This value will suffice to run a

beam energy as high as 54 MeV in the S1 line. The full mechanical, electrical and thermal engineering design is in progress at Elytt Energy in Madrid, Spain.

---

[1] Banerjee, N., *et al. CBETA Design Report.* CBETA Technical Report CBETA-015, Cornell University and Brookhaven National Laboratory (2017).

[2] Bass, R. and J. Crittenden. *Comprehensive Tracking Study for the H-Dipoles and Common Magnets in the Splitter Sections of the Cornell/Brookhaven Energy-Recovery-Linac Test Accelerator.* CBETA Technical Report CBETA-019, CLASSE, Cornell University (2017).

[3] *Opera Simulation Software.* www.operafea.com. Cobham Group.

[4] Crittenden, J. *Splitter Common Magnet Design Issues.* CBETA collaboration meeting (27 July 2017).